beam radiotherapy based on multi-parametric MRI-GTV definition

Ilias Sachpazidis[1,3,*], Panayiotis Mavroidis[4], Constantinos Zamboglou[2,3], Christina Marie Klein[2,3], Anca-Ligia Grosu[2,3], Dimos Baltas[1,3]

[1]Department of Radiation Oncology, Division of Medical Physics, Medical Centre, Faculty of Medicine, University of Freiburg, Germany

[2]Department of Radiation Oncology, Medical Centre, University of Freiburg, Germany

[3]German Cancer Consortium (DKTK) Partner Site Freiburg, German Cancer Research Centre (DKFZ), Heidelberg, Germany

[4]Department of Radiation Oncology, University of North Carolina, Chapel Hill, NC

Category of paper: Full Paper

Running title: Prostate cancer tumour control probability modelling for external beam radiotherapy based on multi-parametric MRI-GTV definition

Keywords: Tumour control probability (TCP), linear-quadratic Poisson model, multivariate logistic regression model, therapy response prediction, prostate cancer

[*]Corresponding author: Ilias Sachpazidis, PhD

Department of Radiation Oncology, Division of Medical Physics, Medical Centre, Faculty of Medicine, University of Freiburg, German

Robert-Koch-Str. 3, 79106, Freiburg, Germany

Tel: +49-761-270-94793, Fax: +49-761-270-95530

Email: Ilias.Sachpazidis@uniklinik-freiburg.de

Abstract:

Purpose: To evaluate the applicability and estimate the radiobiological parameters of linear-quadratic Poisson tumour control probability (TCP) model for primary prostate cancer patients for two relevant target structures (prostate gland and GTV). The TCP describes the dose–response of prostate after definitive radiotherapy (RT). Also, to analyse and identify possible significant correlations between clinical and treatment factors such as planned dose to prostate gland, dose to GTV, volume of prostate and mpMRI-GTV based on multivariate logistic regression model.

Methods: The study included 129 intermediate and high-risk prostate cancer patients (cN0 and cM0), who were treated with image-guided intensity modulated radiotherapy (IMRT) +/- androgen deprivation therapy with a median follow-up period of 81.4 months (range: 42.0 - 149.0) months. Tumour control was defined as biochemical relapse free survival according to the Phoenix definition (BRFS). MpMRI-GTV was delineated retrospectively based on a pre-treatment multi-parametric MR imaging (mpMRI), which was co-registered to the planning CT. The clinical treatment planning procedure was based on prostate gland, delineated on CT imaging modality.

Results: Our results indicated an appropriate α/β = 1.3 Gy for prostate gland and α/β = 2.9 Gy for mpMRI-GTV. Only for prostate gland, *EQD2* and $gEUD_{2Gy}$ were significantly lower in the biochemical relapse (BR) group compared to the biochemical control (BC) group. Fitting results to the linear-quadratic Poisson TCP model for prostate gland and α/β = 1.3 Gy were D_{50} = 66.8 Gy with 95%CI [64.6 Gy, 69.0 Gy], and γ = 3.81 with 95%CI [2.58, 5.20]. For mpMRI-GTV and α/β = 2.9 Gy, D_{50} was 68.1 Gy with 95%CI [66.1 Gy, 70.0 Gy], and γ = 4.45 with 95%CI [3.00, 6.12]. The fitness of the model was better for prostate gland. For the multivariate logistic model, the $gEUD_{2Gy}$ for prostate gland showed a very high significant predictive value (p = 0.001), whereas regarding mpMRI-GTV only its volume showed a significance (p = 0.01).

Conclusion: The linear-quadratic Poisson TCP model was better fit when the prostate gland was considered as responsible target than with mpMRI-GTV. This is compatible with the results of the comparison of the dose distributions among BR and BC groups and with the results achieved with the

multivariate logistic model regarding $gEUD_{2Gy}$. Probably limitations of mpMRI in defining the GTV explain these results. Another explanation could be the relatively homogeneous dose prescription and the relatively low number of recurrences.

I. INTRODUCTION

Advances in radiotherapy treatment and a better understanding of the prostate cancer radiobiology suggest new approaches in dose fractionation to improve prostate cancer control while decreasing radiation induced toxicity. Many studies have compared various radiation delivery regiments e.g. hypofractionated (greater than 2 Gy per fraction) [1] against standard fractionation (1.8 Gy to 2 Gy per fraction) or 3D-CRT vs IMRT [2–6], which indicates that the models and estimation of the model parameters play an important role.

The aim of this study was to investigate the applicability of an established tumour control probability (TCP) model to clinical data of PSA relapse (biochemical relapse) after primary radiation therapy with or without androgen deprivation therapy for prostate cancer. The biochemical recurrence after external radiotherapy was defined according to the Phoenix criteria [7]. The outcome data were analysed considering the 3D-dose distributions in both prostate gland (CT based contours) and GTV as delineated on pre-treatment multi-parametric MRI (mpMRI) in order to investigate the potential relevance of the dose distribution to GTV.

II. METHODS AND MATERIAL

A. Patient cohort and treatment

Our investigation is based on a retrospective, single institution analysis of all patients with localized and histologically proven prostate cancer (PCa) treated with external beam radiotherapy (EBRT) with or without androgen deprivation therapy (ADT) from February 2008 to October 2016, with a minimum follow-up of 36 months. Patients were excluded from the analysis in case of cN1 or cM1 disease, EBRT of the pelvic lymph nodes and initial PSA serum values above 50 ng/ml. A multi-parametric MR

imaging (mpMRI) or PSMA PET/CT at the maximum of 6 months prior to EBRT was mandatory. ADT over 1 month prior to conduction of MRI scans was also an exclusion criterion. The study was approved by the institutional review board. The patient cohort of our investigation included thus a total of 138 patients. The patients' follow-up interval was every 3 to 6 months for the first two years and every 6 to 12 months thereafter with physical examination, PSA measurements and radiological examination if necessary. The Phoenix definition [7] for PSA relapse was used. Detailed description of CTV and PTV definition, of treatment technique and dose parameters for the total groups of patients are available in Zamboglou et al. [5].

From the cohort of 138 patients, 129 had mpMRI prior to EBRT and have been included in current investigation. The median clinical follow-up for the mpMRI group of 129 patients in the current update was 81.4 months (range: 42.0 - 149.0).

Regarding EBRT for the 129 patients, in 32% 3D-conformal and in 68% intensity-modulated RT (IMRT) was delivered as image-guided RT (IGRT) using daily 2D/2D imaging and at least one cone-beam CT per week. Intraprostatic fiducial markers were implanted in 94% of the patients prior to EBRT. The aimed and the planned median prescription dose to the PTV were 76.0 Gy and 74.0 Gy (range: 66.0 – 78.0 Gy), respectively. The median number of fractions was 38 (range: 28 - 42), and the median dose per fraction was 2.0 Gy (range: 1.7 Gy - 2.7 Gy). In our cohort of 129 patients with mpMRI prior to EBRT, 26 have been classified as biochemical relapse (BR) after radiotherapy.

For the purpose of modelling a GTV was delineated retrospectively based on the pre-treatment mpMRI, which was registered to the planning CT. The GTV was contoured by two experienced radiation oncologists in consensus under consideration of the PIRADs v2 criteria [8]. The mpMRI-based GTV was considered as the dominant lesion (DIL) defining the response to the treatment. The mpMRI-GTV volume among all patients was median: 2.65 cc, mean: 3.70 cc, min: 0.25 cc max: 37.97cc, sd: 4.19 cc. The volume of the prostate gland was median: 49.43 cc, mean: 53.10, min: 21.90 cc, max: 187.60 cc and sd: 22.31 cc. Accordingly, the volume fraction of the mpMRI-GTV to the prostate gland was median: 4.9%, mean: 7.5%, min: 0.5%, max: 44.9%, sd: 7.4%.

105 The differential dose volume histograms (DDVH) with a bin width of 0.1 Gy for both mpMRI-GTV and prostate gland have been calculated and exported from Eclipse (Varian, TPS v15.6).

B. The generalized equivalent uniform dose gEUD and $gEUD_{2Gy}$

Given the differential dose volume histogram for a specific dose distribution $\{D\}$ in a volume of interest (VOI) the generalized equivalent uniform dose ($gEUD$) can be computed by the following expression [9,10]:

$$gEUD = gEUD(\{D\}) = \left(\sum_{i=1}^{N}\left(\frac{\boldsymbol{v_i}}{\sum_{\boldsymbol{k=1}}^{\boldsymbol{N}}\boldsymbol{v_k}}\right)D_i^{\alpha}\right)^{1/\alpha} \quad \text{Eq. 1}$$

N is the number of bins of the differential DVH of the corresponding VOI, tumour or organ at risk (OAR), D_i is the dose and v_i is the volume at the i^{th} bin. $\sum_{\boldsymbol{k=1}}^{\boldsymbol{N}}\boldsymbol{v_k} = \boldsymbol{V}$, i.e. the volume of the VOI. Parameter α ($\alpha < 0$ for tumours and $\alpha > 0$ for normal tissues) is the specific parameter that describes the dose-volume effect of the anatomic structure of interest.

$gEUD$ is based on the physical three-dimensional (3D) dose distribution $\{D\}$ and is the dose which when delivered homogeneously to the volume of interest will result in the same biological effect as the inhomogeneous dose distribution described of the underlying DDVH.

To account for the differences in biological effectiveness of the different dose levels at different sampling points within the VOI, the $gEUD_{2Gy}$ quantity can be used [10]. $gEUD_{2Gy}$ uses the 2Gy per fraction equi-effective dose distribution and is calculated in a similar way to $gEUD$ as:

$$gEUD_{2Gy} = \left(\sum_{i=1}^{N}\left(\frac{\boldsymbol{v_i}}{\sum_{\boldsymbol{k=1}}^{\boldsymbol{N}}\boldsymbol{v_k}}\right)EQD2_i^{\alpha}\right)^{1/\alpha} \quad \text{Eq. 2}$$

$EQD2_i$ is the equi-effective dose at 2Gy per fraction of a total dose D_i delivered at d_i dose per fraction for the i^{th} DDVH-bin:

$$EQD2_i = \frac{D_i\left(1 + \frac{d_i}{a/\beta}\right)}{1 + \frac{2\ Gy}{a/\beta}} \quad \text{Eq. 3}$$

α/β in Gy is the fractionation sensitivity parameter of the specific VOI according to the linear-quadratic (LQ) model [11,12].

C. Tumour control probability models

Linear-quadratic Poisson TCP model

Tumour control probability (TCP) models are mathematical formulations to predict the tumour response to radiation therapy on the basis of a dose-response relationship. A widely established formulation for describing this dose-response relationship for tumours is the linear-quadratic Poisson model [13]:

$$P(D) = P(EQD2) = \exp\left(-e^{e\,\gamma-\left(\frac{EQD2}{D_{50}}\right)*(e\,\gamma-\ln\ln 2)}\right) \qquad \text{Eq. 4}$$

P(D) is the tumour control probability, when the tumour is homogenously irradiated at the total dose *D* and *EQD2* is the equi-effective dose at 2Gy per fraction of the total dose *D* when delivered at a fraction dose *d* (see Eq. 3).

D_{50} is the dose in Gy, defined as EQD2, which results in a TCP value of 50% and γ is a dimensionless parameter, defining the maximum normalized value of the dose-response gradient.

For an inhomogeneous dose distribution $\{D\}$ within the tumour of volume *V*, the overall tumour control probability *TCP* is calculated according to:

$$TCP(\{D\},V) = \prod_{i=1}^{N}[P(D_i)]^{v_i/V} \qquad \text{Eq. 5}$$

Or considering Eq. 4 for $P(D_i)$

$$TCP(\{D\},V) = \prod_{i=1}^{N}\left[\exp\left(-e^{e\,\gamma-\left(\frac{EQD2_i}{D_{50}}\right)*(e\,\gamma-\ln\ln 2)}\right)\right]^{v_i/V} \qquad \text{Eq. 6}$$

N is the total number of tumour sub-volumes v_i each of which is assumed to be irradiated homogeneously at the total dose D_i with an equi-effective dose value $EQD2_i$. Since the dose distribution within the tumour $\{D\}$ is commonly described by the differential DVH, in this case *N* is the total number of dose-bins used for the DDVH calculation.

Multivariate logistic regression

In multivariate logistic regression the depending variable (Y) is given as a function of several independent (X_i) variables in the form of:

$$Y = \frac{1}{1 + e^{-(b_0 + \sum b_i X_i)}} \quad \text{Eq. 7}$$

The main null hypothesis of a multivariate logistic regression is that there is no relationship between the X_i variables and the Y variable: H_0: $b_i = 0$, which means that the predicted Y values of the logistic model equation are no closer to the actual Y values than you would expect by chance (if b_i=0 then Y = 1 / (1+1) = 0.5). Putting it another way, in a multivariate logistic regression we are studying if the independent X_i variables have an effect on the probability of obtaining a particular value of the dependent Y variable. TCP can also be described using a multivariate logistic regression model [14,15] where the independent variables, for example, can be the age, the treatment dose, the volume of the target. Accounting for the inhomogeneity of dose distribution in the target volume we consider the equivalent uniform dose $gEUD_{2Gy}$ instead of the physical prescription total treatment dose. Considering both target volumes, prostate gland and GTV, the multivariate logistic regression formulation for TCP (full model) is the following [16]:

$$\mathrm{TCP} = 1 - \mathrm{Y} = \frac{1}{1 + e^{(b_0 + \mathrm{b_1\ gEUD_{2Gy,prostate}} + \mathrm{b_2\ gEUD_{2Gy,GTV}} + \mathrm{b_3\ V_{prostate}} + b_4 V_{GTV})}} \quad \text{Eq. 8}$$

D. Model fitting

The linear-quadratic Poisson TCP model was fitted using the maximum likelihood estimation (MLE) technique. The likelihood function L for the binomial model (response $r = 1$ for relapse-free (BRFS) and 0 for relapse) is:

$$L(P) = L\left(\left(D_{50}, \gamma, \frac{\alpha}{\beta}\right), (\{D\}, V)\right) = \prod_{j=1}^{N} P_j{}^{r_j} . (1 - P_j)^{(1-r_j)} \qquad \text{Eq. 9}$$

with P_j the TCP prediction, r_j the binary clinical response for the j-th patient and N the total number of patients in the study. The best parameter estimation for D_{50} and γ are those maximizing the $L(P)$ estimator or equivalently minimizing the $LL = -ln(L(P))$:

$$minimize\,\{LL\} = minimize\{-\sum_{j=1}^{M}\{r_j \ln(P_j) + (1 - r_j)\ln(1 - P_j)\}\} \qquad \text{Eq. 10}$$

For the optimization we used simulated annealing (SA), a stochastic solver as implemented in open source "*Object Oriented Optimization Toolbox*" .NET library [17] . The estimation of the confidence interval (CI) for the parameter values was based on the likelihood profiling method, without assuming normality of the maximum likelihood estimator [18].

For the multivariate logistic regression model, the glm() fitting function and stepwise selection stepAIC() function, in both directions, as provided by R version 3.5.3 [19,20] were used. Akaike Information Criterion (AIC) was considered to measure the relative quality of the nested models in multivariate analysis [21,22].

E. Goodness-of-fit

For the goodness-of-fit of our models, the Hosmer-Lemeshow (HL) test [23] was performed to test the hypothesis that the predictions agree well with the observed outcomes, in which a p value of greater than 0.05 indicates good agreement [24]. A group parameter value of $g = 10$ was used. HL test performed with *ResourceSelection* package [25] in R version: 3.5.3.

F. Model parameter values and assumptions

For the TCP model fitting and for the mpMRI-GTV and prostate gland α/β values in the range of 0.1 Gy to 20.0 Gy have been considered. For the generalized equivalent uniform dose $gEUD_{2Gy}$, a value of α = -10 was applied [10] for both target types; prostate gland and GTV. Plots created in Python 3.7.7 with matplotlib (v3.1.3), numpy (1.18.1), pandas (1.0.3), rpy2 (2.9.4) libraries. All statistical comparisons were performed with Wilcoxon rank sum nonparametric test (R package stats version 3.6.2) with a significance level (alpha) of 0.05.

III. RESULTS

A. Comparison of dose values in prostate gland and GTV

We compared the minimum physical dose for mpMRI-GTV and prostate gland for the biochemical control (BC), defined by BRFS, and biochemical relapse (BR) groups. For the BC group the median of the minimum dose in the prostate gland was 72.3 Gy (range 49.7 Gy – 77.7 Gy) whereas in the mpMRI-GTV it was 73.5 Gy (range 63.4 Gy – 78.4 Gy). For the BR group the median of the minimum dose was 71.3 Gy (range 54.2 Gy – 76.1 Gy) and 72.7 Gy (range 53.7 Gy – 76.0 Gy) for the prostate gland and mpMRI-GTV respectively.

As illustrated in Fig. 1, the minimum physical dose between the two groups is significantly different for prostate gland ($p = 0.0345$) but not for mpMRI-GTV ($p = 0.0728$).

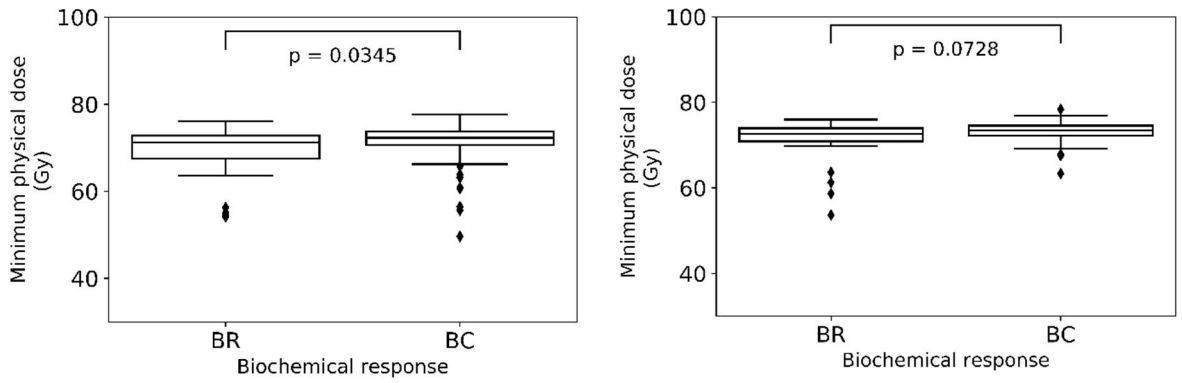

Figure 1: Boxplots for the minimum physical dose for prostate gland (left, $p = 0.0345$) and mpMRI-GTV (right, $p = 0.0728$) for the biochemical control (BC) and biochemical relapse (BR) groups.

Regarding EUD and BC group the median value for the prostate gland was 75.5 Gy (range 68.3 Gy – 79.8 Gy) whereas for the mpMRI-GTV it was 75.3 Gy (range 69.8 Gy – 79.7 Gy). For the BR group the median EUD was 74.5 Gy (range 65.5 Gy – 77.2 Gy) and 74.5 Gy (range 65.6 Gy – 77.0 Gy) for the prostate gland and mpMRI-GTV respectively.

Figure 2 illustrates the results of the comparison of equivalent uniform dose for prostate gland and mpMRI-GTV. No significant differences between the two groups and for both target types were showed: for prostate gland $p = 0.0859$ and for mpMRI-GTV $p = 0.1597$.

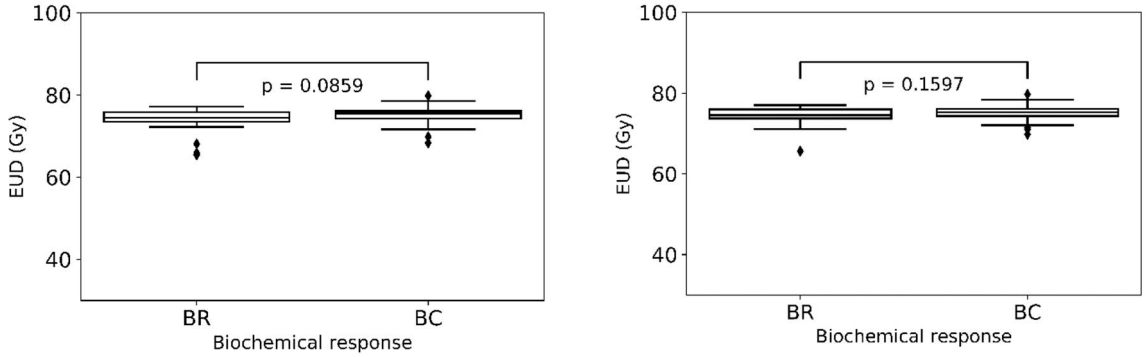

Figure 2: Boxplots for the EUD for prostate gland (left) and mpMRI-GTV (right) for the biochemical relapse (BR) and biochemical control (BC) groups.

Furthermore, we compared the minimum EQD2 dose value for the two target types, mpMRI-GTV and prostate gland, for the biochemical relapse (BR) and biochemical control (BC) groups. As it will be discussed later and based on the linear-quadratic Poisson TCP model fitting, the most appropriate α/β value was 1.3 Gy and 2.9 Gy for prostate gland and mpMRI-GTV, respectively.

For the BC group the median of the minimum EQD2 in the prostate gland was 70.6 Gy (range 43.0 Gy – 82.2 Gy) compared to 72.9 Gy (range 57.5 Gy – 79.3 Gy) for the mpMRI-GTV, and for the BR group it was 68.7 Gy (range 43.0 – 77.3 Gy) and 72.1 Gy (range 46.1 Gy – 76.8 Gy) respectively.

Figure 3 illustrates the boxplot of the minimum dose as EQD2 in mpMRI-GTV and prostate gland. Similarly to the analysis for the minimum physical dose (Figure 1), significantly lower minimum EQD2 values were observed in the BR group compared to the BC group only for prostate gland ($p = 0.0326$).

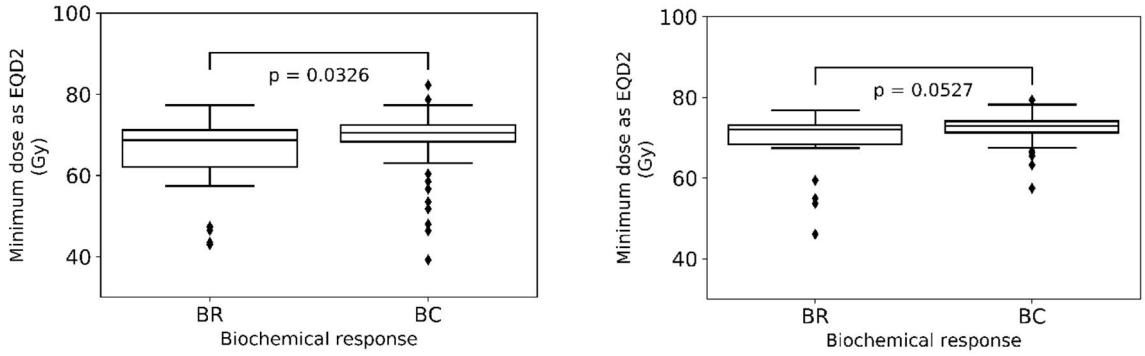

Figure 3: Boxplots of the minimum dose as EQD2 for prostate gland with $\alpha/\beta = 1.3$ Gy (left) and mpMRI-GTV with $\alpha/\beta = 2.9$ Gy (right) for the biochemical relapse (BR) and biochemical control (BC) groups.

The median $gEUD_{2Gy}$ for the two target types, prostate gland and mpMRI-GTV, was 75.3 Gy (range 63.9 Gy – 86.1 Gy) and 75.3 Gy (range 68.9 Gy – 81.6 Gy) for the BR group and 74.5 Gy (range 58.5 Gy – 79.1 Gy) and 74.3 Gy (range 60.3 Gy – 78.2 Gy) for the BC group, accordingly.

When comparing the $gEUD_{2Gy}$ values for the two response groups (BR and BC) and the two target types, prostate gland and GTV, only for the prostate gland, a significantly lower $gEUD_{2Gy}$ value in the BR group could be demonstrated (p = 0.0482, Figure 4). This is in alignment with our previous findings for EQD2 and physical dose.

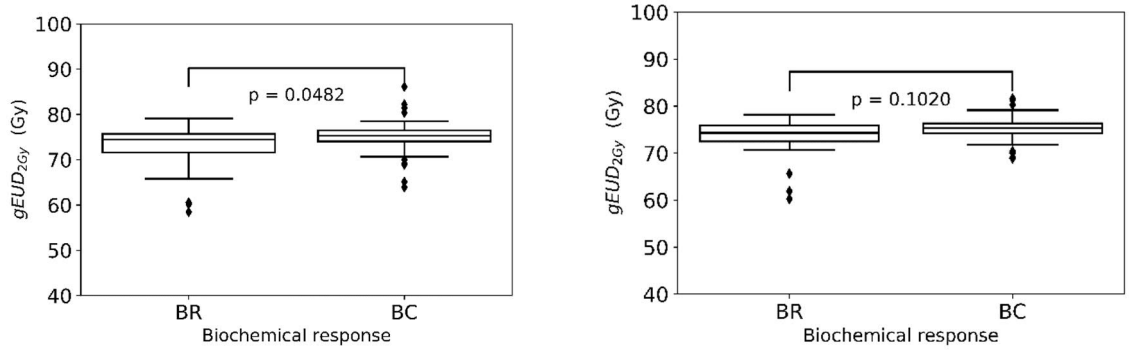

Figure 4: Boxplots of the generalized equivalent uniform dose, $gEUD_{2Gy}$, for prostate gland (left) with α/β = 1.3 Gy and mpMRI-GTV (right) with α/β = 2.9 Gy for the biochemical relapse (BR) and biochemical control (BC) groups.

B. Linear-quadratic Poisson TCP model fitting

Due to the fact that there was no adequate variability in the fraction scheme of the clinical data considered, it was not possible to fit the models with an acceptable 95% CI when α/β was considered as a free variable to be fitted. For this reason, we investigated the behaviour of *LL* estimator values for α/β in the region of 0.1 Gy to 20.0 Gy. The results are shown in figure 5. The minimum *LL* values are observed for an α/β = 1.3 Gy when the prostate gland is considered as a target and α/β = 2.9 Gy when mpMRI-GTV is considered as the target defining the biological response. For a fine estimation of the minimum optimized *LL* value an α/β step of 0.1 Gy was considered. The fitness of the TCP model considering the prostate gland as underlying target is better than when mpMRI-GTV is considered as target: lower *LL* value is demonstrated for prostate gland than the mpMRI-GTV (Table 1): 60.02 *vs* 61.17. Evaluating the goodness-of-fit of the linear-quadratic Poisson TCP model using the Hosmer-Lemeshow (HL) test showed no significant difference between the observed and the predicted outcomes for both target types where for prostate gland the *HL* test showed $p = 0.66$ ($X^2 = 5.92$) and for mpMRI-GTV a $p = 0.54$ ($X^2 = 7.00$).

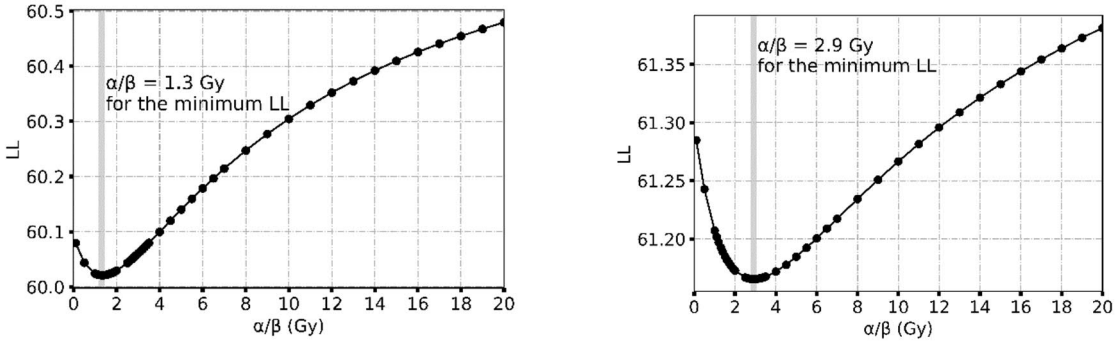

Figure 5: Plot of optimized *LL* (Eq. 12) against α/β when prostate gland (left) and mpMRI-GTV (right) are considered as the target causing the observed response.

In the following analysis we assume for the two different target types, prostate gland and mpMRI-GTV, the above mentioned individual α/β values. For this case, the results of *LL*-based model fitting for the two target types are summarized in table 1. For the TCP model based on prostate gland slightly lower D_{50} value and lower γ value than for mpMRI-GTV were estimated.

Table 1: Fitted clinical data to linear-quadratic Poisson TCP model for the two different target types for intermediate and high-risk prostate cancer patients, for the best estimated α/β values (Fig. 5).

Target type	***D_{50}* (Gy) [95%CI]**	***γ* [95%CI]**	***α/β* (Gy)**	***LL***	***HL test***
prostate gland	66.8 [64.6, 69.0]	3.81 [2.58, 5.20]	1.3	60.02	$p = 0.66$ ($X^2 = 5.92$)
mpMRI-GTV	68.1 [66.1, 70.0]	4.45 [2.99, 6.12]	2.9	61.17	$p = 0.54$ ($X^2 = 7.00$)

The TCP predictions for the linear-quadratic Poisson TCP model for the two different target types in conjunction to EQD2 for homogeneous dose distribution are shown in Fig. 6.

The model predictions for TCP 90% and 95% biochemical response are for EQD2 values of homogeneous dose delivery of 78.6 Gy with 95% CI [73.1 Gy, 86.7 Gy] and 83.1 Gy with 95% CI [76.3 Gy, 93.4 Gy], respectively, when the prostate gland is considered as the responsible target. These values are slightly different when the mpMRI-GTV is considered as the target: 78.4 Gy with 95% CI [73.5 Gy, 85.6 Gy] and 82.4 Gy with 95% CI [76.3 Gy, 91.5 Gy], respectively.

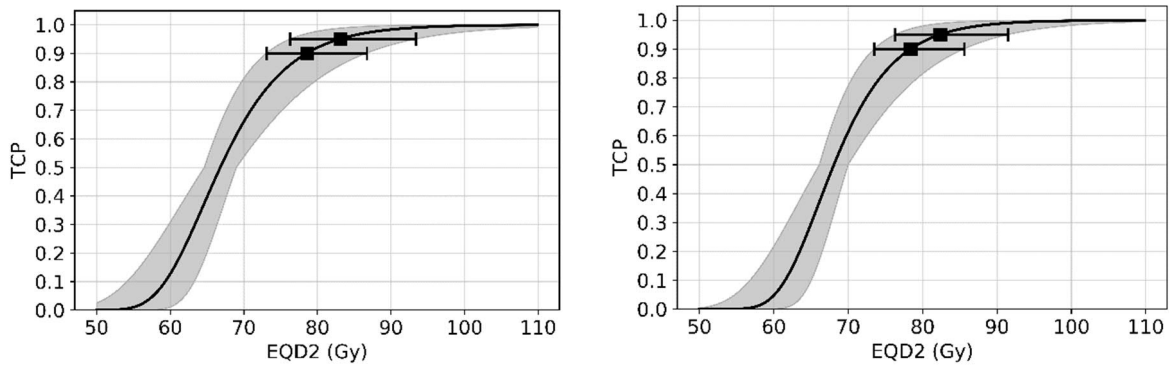

Figure 6: Response curves of linear-quadratic Poisson model for prostate gland with $\alpha/\beta = 1.3$ Gy (left) and for mpMRI-GTV with $\alpha/\beta = 2.9$ Gy (right). Grey area represents the 95% CI. The predicted *EQD2* values and their 95%-CI for 90% and 95% TCP levels are also shown.

The absolute difference of the TCP predictions of both linear-quadratic Poisson fitted models is shown in Fig. 7. For homogeneous dose delivery with *EQD2* values above 74.6 Gy (TCP ~ 0.81) both model predictions agree within 1%. The maximum TCP deviation (0.11) among the two models is observed for *EQD2* of 63.3 Gy.

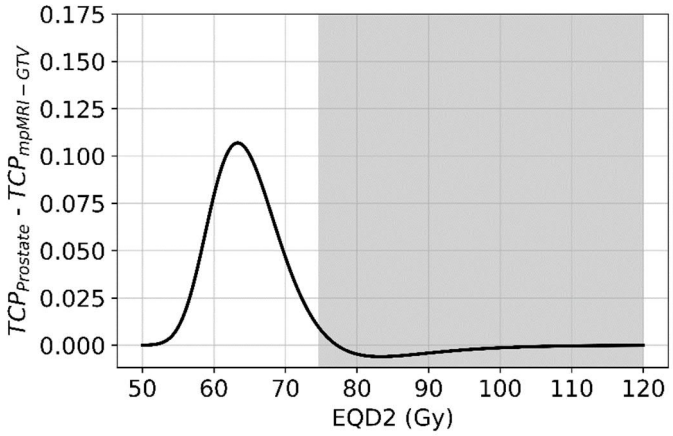

Figure 7: Absolute difference in predicted TCP values for the linear-quadratic Poisson model fitted for prostate gland ($TCP_{prostate}$) and for mpMRI-GTV ($TCP_{mpMRI-GTV}$). For *EQD2* above 74.6 Gy the absolute differences in TCP stay below 1%.

C. Multivariate logistic TCP model fitting

For the multivariate logistic model, the full model (Eq. 9) was used. As stated previously the $gEUD_{2Gy}$ for prostate gland was calculated with α/β = 1.3 Gy, and for mpMRI-GTV with α/β = 2.9 Gy. The best fitted nested model, after the stepwise analysis in both directions, showed only the $gEUD_{2Gy}$ in prostate gland (p = 0.001) and the volume of mpMRI-GTV (p = 0.01) to be significant. The coefficients of the multivariate logistic model were: b_0 = 11.883 with 95% CI [3.520, 21.637], b_1 = -0.18 (Gy^{-1}) with 95% CI [-0.32, -0.07], b_4 = 0.127 (cc^{-1}) with 95% CI [0.025, 0.256].

The goodness-of-fit as described by the *HL* test showed no significant difference between the observed and the predicted outcomes for the multivariate logistic model with p = 0.26 (X^2 = 9.97).

IV. DISCUSSION

The analysis of minimum physical dose, minimum *EQD2* and $gEUD_{2Gy}$ demonstrated significant lower values to the BR than to BC response group only for prostate gland. This is in alignment with the results of the multivariate logistic TCP model, demonstrating a significant predictive value only for the dose distribution in prostate gland expressed as $gEUD_{2Gy}$.

The analysis of *LL* fitness of the linear-quadratic Poisson TCP model in dependence on the assumed α/β value indicated two different α/β values as appropriate for the investigated target volume types: A very low α/β value of 1.3 Gy for prostate gland and a low α/β value of 2.9 Gy for mpMRI-GTV. This indicates lower fractionation sensitivity for the mpMRI-GTV when this is considered to define the clinical response when compared to prostate gland.

Levegrün et al. 2001 [26] fitted TCP models with the maximum likelihood method to biopsy outcome from 103 prostate cancer patients with a minimum follow-up of 30 months, after 3D-CRT, using an α/β = 10.0 Gy and alternatively an α/β = 1.5 Gy. For their model fitting process individual DVHs for the planning target volume (PTV) recalculated for EQD2 have been used. Their results for α/β = 1.5 Gy were worse in terms of maximum likelihood values compared to the fitting results for α/β = 10.0 Gy for the low-, intermediate- and high-risk sub-groups. The estimated TCP model parameter values for D_{50} and γ_{50} for α/β = 10.0 Gy were 65.0 Gy and 2.93 (γ = 3.24) in the low-risk group, 67.8 Gy and 3.60 (γ = 3.96) in the intermediate-risk group and finally 75.7 Gy and 3.33 (γ = 3.67) in the high-risk group, respectively.

In contrast, we showed that for our cohort the linear-quadratic Poisson TCP model fits better for low α/β values (Fig. 5). The estimated D_{50} value of 66.8 Gy for our mixed intermediate- and high-risk cohort is lower than the corresponding values for those two risk groups in Levegrün's publication. Our γ value of 3.81 lies in between the reported values for the two risk groups demonstrating similar steep TCP curves.

The differences observed in D_{50} values can be probably explained by the fact that Levegrün et al. used the PTV as responsible target which significantly overestimates the prostate gland due to the

implemented setup margin of 10 mm [26,27] and the higher assumed α/β value of 10.0 Gy compared to our estimation of 1.3 Gy for the prostate gland.

Fowler [28] published in 2005 a linear-quadratic logit model for 5-year biochemical control for intermediate risk prostate cancer patients, based on the prescription doses for prostate as given in the considered clinical data. Fowler estimated D_{50} = 65.6 Gy and γ_{50} = 2.1 (γ = 2.36) for α/β = 1.5 Gy. Both values reported by Fowler, D_{50} and steepness of the dose response curve as described by γ, are lower compared to our results for prostate gland (D_{50} = 66.8 Gy and γ = 3.81, Table 1). This is also the case when Fowler´s results are compared to the results by Levegrün et al. [26] for the intermediate-risk group. It must be pointed out that Fowler considered the prescription dose for his analysis whereas in the current study and in the paper by Levegrün et al. the individual planned DVHs for the target volumes have been utilized.

For our patient cohort the resulted variation for the minimum physical dose, *EUD*, minimum *EQD2* and $gEUD_{2Gy}$ for prostate gland were 28.0 Gy, 14.4 Gy, 43.0 Gy, 27.7 Gy accordingly. The observed variation in minimum physical dose of 28.0 Gy is much higher (factor of 2.3) than the range of planned prescription dose of 12.0 Gy (66.0 to 78.0 Gy). Since the minimum dose in the target dominates the TCP, it is obvious that using the prescription dose for TCP modelling is a problematic simplification and biases the TCP model fitting expecting an underestimation of the steepness of the response curve.

The clinical results observed in our study can be better described by the linear-quadratic Poisson TCP model fitted to the dose distributions in the prostate gland than in mpMRI-GTV (*LL* = 60.02 for prostate gland versus *LL* = 61.17 for mpMRI-GTV).

This observation together with the failure to demonstrate significant differences in dosimetric parameters among BR and BC response groups when mpMRI-GTV is assumed as the responsible target could be explained by limitations of mpMRI to identify the true cancer volume in the prostate. As discussed by Zamboglou el al., a better predictor of the biochemical response is the union region defined by mpMRI and PSMA PET [5]. This is also supported by intraindividual comparison studies between mpMRI, PSMA PET and histopathology reference [29–32]. All these studies concluded that PSMA-

PET provides superior detection of intraprostatic tumour lesions with better sensitivity than mpMRI. Thus, PSMA-PET/CT can be used to enhance mpMRI to provide improved detection and even characterization [33] of lesions.

Other probable explanations for these observations could be the limited number of 129 patients in our cohort, the low number of the observed failures (20 %) and the relatively homogeneous dose per fraction in the range 1.7 to 2.7 Gy.

V. CONCLUSIONS

In our study we observed 129 prostate cancer patients, who were treated with image-guided intensity modulated radiotherapy with a median clinical follow-up of 81.4 months (range: 42.0 - 149.0). We estimated the radiobiological parameters of the linear-quadratic Poisson TCP model for prostate cancer patients for two relevant target structures, prostate gland and mpMRI-GTV. The model fits better to the clinical BRFS results when the prostate gland and not the mpMRI-GTV is considered as the underlying target and indicates a very low α/β = 1.3 Gy and a relative steep dose response curve (γ = 3.81). A probable explanation could be limitations in defining GTV using mpMRI. This is also supported by the results of comparison of the dosimetric parameter values in both target types regarding biochemical response and by the fitting results of the multivariate logistic model.

VI. ABBREVIATIONS

{D}: dose distribution

3D: three-dimensional

3D-CRT: three-dimensional conformal radiation therapy

95%CI: 95% confidence interval

ADT: androgen deprivation therapy

BC: biochemical control group

BFRS: biochemical relapse free survival according to the Phoenix definition

BR: biochemical relapse group

CT: computed tomography

DDVH: differential dose volume histograms

DIL: dominant lesion

EBRT: external beam radiation therapy

EQD2: equi-effective dose at 2Gy per fraction

gEUD: generalized equivalent uniform dose

GTV: gross tumour volume

HL test: Hosmer-Lemeshow goodness-of-fit test

IGRT: image-guided radiotherapy

IMRT: intensity-modulated radiation therapy

LL: log likelihood

LQ: linear quadratic model

mpMRI: multi-parametric MRI

MRI: magnetic resonance imaging

p: p-value for statistical hypothesis testing

PCa: prostate cancer

PET: positron emission tomography

PSA: prostate-Specific Antigen (test)

PSMA: prostate-specific membrane antigen

PTV: planning target volume

RT: radiotherapy

sd: standard deviation

TCP: tumour control probability

VOI: volume of interest

α/β: The ratio of ‘‘intrinsic radiosensitivity’’ to ‘‘repair capability’’ of a specified tissue

VII. DECLARATIONS

A. Ethical Approval and Consent to participate

Written informed consent for participation was obtained from all participants.

B. Consent for publication

This work has been read and approved by all authors. Written informed consent for publication was obtained from all participants.

C. Availability of supporting data

The datasets used and/or analyses during the current study are available from the corresponding author on reasonable request.

D. Competing interests

The authors declare that they have no competing interests.

E. Funding

The study was funded from house internal budget.

F. Authors' contributions

IS, CZ, ALG, and DB analysed interpreted the data. IS and PM performed the statistical analysis and were contributors in writing the manuscript. CZ and CK generated the mpMRI-GTVs (data acquisition, data delineation). IS, PM and DB were responsible for biological modelling. DB supervised the whole project. All authors read and approved the final manuscript.

G. Acknowledgements

Not applicable.

VIII. REFERENCES

[1] Vogelius IR, Bentzen SM. Dose Response and Fractionation Sensitivity of Prostate Cancer After External Beam Radiation Therapy: A Meta-analysis of Randomized Trials. International journal of radiation oncology, biology, physics 2018;100(4):858–65, doi:10.1016/j.ijrobp.2017.12.011.

[2] Hernández TG, González AV, Peidro JP, Ferrando JVR, González LB, Cabañero DG, Torrecilla JL. Radiobiological comparison of two radiotherapy treatment techniques for high-risk prostate cancer. Reports of practical oncology and radiotherapy journal of Greatpoland Cancer Center in Poznan and Polish Society of Radiation Oncology 2013;18(5):265–71, doi:10.1016/j.rpor.2012.12.006.

[3] Wang L, Li C, Meng X, Li C, Sun X, Shang D, Pang L, Li Y, Lu J, Yu J. Dosimetric and Radiobiological Comparison of External Beam Radiotherapy Using Simultaneous Integrated Boost Technique for Esophageal Cancer in Different Location. Front. Oncol. 2019;9:674, doi:10.3389/fonc.2019.00674.

[4] Mesbahi, Rasouli, Mohammadzadeh, Nasiri Motlagh, Ozan Tekin. Comparison of Radiobiological Models for Radiation Therapy Plans of Prostate Cancer: Three-dimensional Conformal versus Intensity Modulated Radiation Therapy. Journal of biomedical physics & engineering 2019;9(3):267–78, doi:10.31661/jbpe.v9i3Jun.655.

[5] Zamboglou C, Klein CM, Thomann B, Fassbender TF, Rischke HC, Kirste S, Henne K, Volegova-Neher N, Bock M, Langer M, Meyer PT, Baltas D, Grosu AL. The dose distribution in dominant intraprostatic tumour lesions defined by multiparametric MRI and PSMA PET/CT correlates with the outcome in patients treated with primary radiation therapy for prostate cancer. Radiation oncology (London, England) 2018;13(1):65, doi:10.1186/s13014-018-1014-1.

[6] Zamboglou C, Thomann B, Koubar K, Bronsert P, Krauss T, Rischke HC, Sachpazidis I, Drendel V, Salman N, Reichel K, Jilg CA, Werner M, Meyer PT, Bock M, Baltas D, Grosu AL. Focal

dose escalation for prostate cancer using 68Ga-HBED-CC PSMA PET/CT and MRI: a planning study based on histology reference. Radiation oncology (London, England) 2018;13(1):81, doi:10.1186/s13014-018-1036-8.

[7] Roach M, Hanks G, Thames H, Schellhammer P, Shipley WU, Sokol GH, Sandler H. Defining biochemical failure following radiotherapy with or without hormonal therapy in men with clinically localized prostate cancer: recommendations of the RTOG-ASTRO Phoenix Consensus Conference. International journal of radiation oncology, biology, physics 2006;65(4):965–74, doi:10.1016/j.ijrobp.2006.04.029.

[8] Jordan EJ, Fiske C, Zagoria R, Westphalen AC. PI-RADS v2 and ADC values: is there room for improvement? Abdominal radiology (New York) 2018;43(11):3109–16, doi:10.1007/s00261-018-1557-5.

[9] Zhou S-M, Das S, Wang Z, Marks LB. Relationship between the generalized equivalent uniform dose formulation and the Poisson statistics-based tumor control probability model. Medical physics 2004;31(9):2606–09, doi:10.1118/1.1783532.

[10] Allen Li X, Alber M, Deasy JO, Jackson A, Ken Jee K-W, Marks LB, Martel MK, Mayo C, Moiseenko V, Nahum AE, Niemierko A, Semenenko VA, Yorke ED. The use and QA of biologically related models for treatment planning: short report of the TG-166 of the therapy physics committee of the AAPM. Medical physics 2012;39(3):1386–409, doi:10.1118/1.3685447.

[11] Fowler JF. 21 years of biologically effective dose. The British journal of radiology 2010;83(991):554–68, doi:10.1259/bjr/31372149.

[12] Fowler JF. Sensitivity analysis of parameters in linear-quadratic radiobiologic modeling. International journal of radiation oncology, biology, physics 2009;73(5):1532–37, doi:10.1016/j.ijrobp.2008.11.039.

[13] El Naqa I. A Guide to Outcome Modeling in Radiotherapy and Oncology: Listening to the Data. Series in Medical Physics and Biomedical Engineering Ser. Milton: Chapman and Hall/CRC; 2018.

[14] Bentzen S, Harari P, Tome W, Mehta M, editors. Radiation oncology advances ;: S.M. Bentzen … [et al.](Eds.). Cancer Treatment and Research, 139. USA: Springer; 2008.

[15] Naqa IE, Deasy JO, Mu Y, Huang E, Hope AJ, Lindsay PE, Apte A, Alaly J, Bradley JD. Datamining approaches for modeling tumor control probability. Acta Oncologica 2010;49(8):1363–73, doi:10.3109/02841861003649224.

[16] Levegrün S, Jackson A, Zelefsky MJ, Venkatraman ES, Skwarchuk MW, Schlegel W, Fuks Z, Leibel SA, Ling CC. Risk group dependence of dose–response for biopsy outcome after three-dimensional conformal radiation therapy of prostate cancer. Radiotherapy and Oncology 2002;63(1):11–26, doi:10.1016/s0167-8140(02)00062-2.

[17] Matt Campbell. OOOT: Object-Oriented Optimization Toolbox; 2020. Available from: https://github.com/DesignEngrLab/OOOT.

[18] Mavroidis P, Tzikas A, Papanikolaou N, Lind BK. Toolkit for determination of dose-response relations, validation of radiobiological parameters and treatment plan optimization based on radiobiological measures. Technology in cancer research & treatment 2010;9(5):523–37, doi:10.1177/153303461000900511.

[19] Venables WN, Ripley BD. Modern Applied Statistics with S. 4th ed. Statistics and computing. New York: Springer; 2010.

[20] Dobson AJ, Barnett A. An Introduction to Generalized Linear Models, Third Edition. 3rd ed. Chapman & Hall / CRC Texts in Statistical Science. Hoboken: CRC Press; 2008.

[21] Gelman A, Hill J. Data Analysis Using Regression and Multilevel/Hierarchical Models. Cambridge: Cambridge University Press; 2006.

[22] Agresti A. Categorical Data Analysis. 3rd ed. Wiley Series in Probability and Statistics. Hoboken: Wiley; 2014.

[23] Hosmer DW, Lemeshow S, Sturdivant RX. Applied logistic regression. 3rd ed. Wiley Series in Probability and Statistics. Hoboken: Wiley; 2013.

[24] Wang Z, Chen M, Sun J, Jiang S, Wang L, Wang X, Sahoo N, Gunn GB, Frank SJ, Nguyen Q-N, Liao Z, Chang JY, Zhu XR, Zhang X. Lyman-Kutcher-Burman normal tissue complication probability modeling for radiation-induced esophagitis in non-small cell lung cancer patients receiving proton radiotherapy. Radiotherapy and oncology journal of the European Society for Therapeutic Radiology and Oncology 2020;146:200–04, doi:10.1016/j.radonc.2020.03.003.

[25] Sólymos P, Lele SR. Revisiting resource selection probability functions and single-visit methods: clarification and extensions. Methods Ecol Evol 2016;7(2):196–205, doi:10.1111/2041-210X.12432.

[26] Levegrün S, Jackson A, Zelefsky MJ, Skwarchuk MW, Venkatraman ES, Schlegel W, Fuks Z, Leibel SA, Ling CC. Fitting tumor control probability models to biopsy outcome after three-dimensional conformal radiation therapy of prostate cancer: pitfalls in deducing radiobiologic parameters for tumors from clinical data. International journal of radiation oncology, biology, physics 2001;51(4):1064–80.

[27] Levegrün S, Jackson A, Zelefsky MJ, Venkatraman ES, Skwarchuk MW, Schlegel W, Fuks Z, Leibel SA, Ling CC. Analysis of biopsy outcome after three-dimensional conformal radiation therapy of prostate cancer using dose-distribution variables and tumor control probability models. International Journal of Radiation Oncology*Biology*Physics 2000;47(5):1245–60, doi:10.1016/s0360-3016(00)00572-1.

[28] Fowler JF. The radiobiology of prostate cancer including new aspects of fractionated radiotherapy. Acta Oncologica 2005;44(3):265–76, doi:10.1080/02841860410002824.

[29] Eiber M, Weirich G, Holzapfel K, Souvatzoglou M, Haller B, Rauscher I, Beer AJ, Wester H-J, Gschwend J, Schwaiger M, Maurer T. Simultaneous 68Ga-PSMA HBED-CC PET/MRI Improves the Localization of Primary Prostate Cancer. European urology 2016;70(5):829–36, doi:10.1016/j.eururo.2015.12.053.

[30] Bettermann AS, Zamboglou C, Kiefer S, Jilg CA, Spohn S, Kranz-Rudolph J, Fassbender TF, Bronsert P, Nicolay NH, Gratzke C, Bock M, Ruf J, Benndorf M, Grosu AL. 68Ga-PSMA-11 PET/CT and multiparametric MRI for gross tumor volume delineation in a slice by slice analysis with whole mount histopathology as a reference standard - Implications for focal radiotherapy planning in primary prostate cancer. Radiotherapy and oncology journal of the European Society for Therapeutic Radiology and Oncology 2019;141:214–19, doi:10.1016/j.radonc.2019.07.005.

[31] Hicks RM, Simko JP, Westphalen AC, Nguyen HG, Greene KL, Zhang L, Carroll PR, Hope TA. Diagnostic Accuracy of 68Ga-PSMA-11 PET/MRI Compared with Multiparametric MRI in the Detection of Prostate Cancer. Radiology 2018;289(3):730–37, doi:10.1148/radiol.2018180788.

[32] Berger I, Annabattula C, Lewis J, Shetty DV, Kam J, Maclean F, Arianayagam M, Canagasingham B, Ferguson R, Khadra M, Ko R, Winter M, Loh H, Varol C. 68Ga-PSMA PET/CT vs. mpMRI for locoregional prostate cancer staging: correlation with final histopathology. Prostate cancer and prostatic diseases 2018;21(2):204–11, doi:10.1038/s41391-018-0048-7.

[33] Zamboglou C, Carles M, Fechter T, Kiefer S, Reichel K, Fassbender TF, Bronsert P, Koeber G, Schilling O, Ruf J, Werner M, Jilg CA, Baltas D, Mix M, Grosu AL. Radiomic features from PSMA PET for non-invasive intraprostatic tumor discrimination and characterization in patients with intermediate- and high-risk prostate cancer - a comparison study with histology reference. Theranostics 2019;9(9):2595–605, doi:10.7150/thno.32376.